

Ideal performance of cascade and noncascade intersubband and interband long-wavelength semiconductor lasers

Michael E. Flatté^{a)} and J. T. Olesberg

Department of Physics and Astronomy and Optical Science and Technology Center, University of Iowa, Iowa City, Iowa 52242

C. H. Grein

Department of Physics, University of Illinois, Chicago, Illinois 60607

(Received 21 December 1998; accepted for publication 10 August 1999)

The ideal performance of cascade and noncascade intersubband and interband laser active regions is directly compared in a cavity-insensitive way. For devices not limited by series resistance or series voltage (such as can in principle be accomplished by cascading) the relevant figure of merit is the net material gain per unit volumetric power dissipation density in the active region. This figure of merit is evaluated at 77 and 300 K for a variety of structures relying on interband and intersubband transitions, each of which may constitute the active region of a cascade or noncascade device. A design for an 11 μm laser active region is proposed whose ideal performance exceeds that of current intersubband lasers. © 1999 American Institute of Physics. [S0003-6951(99)05140-2]

Many of the challenges associated with the design of semiconductor laser diodes become more severe at longer wavelengths. These include a reduced carrier lifetime associated with the Auger recombination process, which (qualitatively) depends exponentially on the emission wavelength, and the difficulty of confining the larger optical mode within an epilayer of reasonable thickness. At this time there are two principal types of semiconductor laser diodes that operate in the long-wavelength infrared (LWIR, $\lambda \sim 8\text{--}12\ \mu\text{m}$): lead-salt lasers¹ and quantum cascade intersubband lasers^{2,3} based on the InP material system. In contrast, in the mid-wavelength infrared (MWIR, $\lambda \sim 2\text{--}5\ \mu\text{m}$) there are several types of traditional (noncascade) III-V semiconductor lasers. Of the material systems these lasers are based on, only the InAs/GaInSb material system^{4,5} can in principle produce an 8–12 μm laser. The longest-wavelength laser⁶ demonstrated to date, however, emits at 5.2 μm at 185 K.

It has been argued recently that thin ($\sim 200\text{--}400\ \text{\AA}$) noncascade active regions in the MWIR based on the InAs/GaInSb material system could generate sufficient gain for lasing, so long as they were embedded in a separate confinement region (SCR).⁷ This argument was based on direct calculations of a figure of merit of the active region that, for a given cavity design, determines the threshold current density: the net material gain per unit volumetric current.⁸

This letter extends the consideration of such structures to the long-wavelength infrared, and also generalizes the figure of merit so that active regions based on intersubband transitions, which have typically formed the heart of quantum cascade lasers, may be compared directly with active regions based on interband transitions, which are commonly used in noncascade lasers. The basis for comparison is evaluating which system will require the lowest input electrical power to generate a given output optical power. This is thus a more general comparison than that of Ref. 9.

We are led to consider a new figure of merit: the net material gain per unit volumetric *power dissipation* in the active region. To justify this we consider the input power density (P_i/A) in the device to come from an active region term, a series voltage term, and a series resistance term

$$\frac{P_i}{A} = IV_{\text{AR}} + IV_s + I^2\rho_s, \quad (1)$$

where I is the areal current density, V_{AR} is the voltage across the active region, V_s is the series voltage and ρ_s is the series resistivity. We note that the series resistance and voltage terms for *either* interband¹⁰ or intersubband lasers can in principle be reduced to an insignificant level relative to the active region term by improving the properties of the material system, or if that has reached a mature limit, by cascading.

We will therefore focus on guidelines for choosing an active region which is as efficient as possible at generating light for a given input power density to the active region ($P_{\text{AR}}/A = IV_{\text{AR}}$). The dependence of the active region power on the net material gain per unit volumetric power dissipation density can be seen by writing P_{AR} for a given optical output power (P_o) as

$$P_{\text{AR}} = \frac{AD_{\text{mode}}(\alpha_m + \langle\alpha_w\rangle)}{\eta_i} \left(\frac{P}{\gamma - \alpha_a} \right) + \frac{P_o(\alpha_m + \langle\alpha_w\rangle)}{\alpha_m} \left(\frac{\gamma}{\gamma - \alpha_a} \right) \frac{1}{\eta_i} \left[\frac{eV_o}{h\nu} \right]. \quad (2)$$

Here A is the area (length times width) of the laser stripe, γ is the material gain, α_m is the mirror loss, $\langle\alpha_w\rangle$ is the non-active region modal loss in the waveguide (e.g., free carrier absorption in the doped clads), α_a is the material loss in the active region, η_i is the injection efficiency, D_{mode} is the width of the optical mode, e is the electron charge, and $h\nu$ is the emitted photon energy. V_o is, for cascade structures, the voltage drop across a single stage of the cascade, and for noncascade structures $V_o = V_{\text{AR}}$.

^{a)}Electronic mail: flatte@rashi.physics.uiowa.edu

TABLE I. Results for ideal laser active region designs for six systems at room temperature: band gap E_g , maximum net gain per unit volumetric power dissipation density $[(\gamma - \alpha_a)/P]_{\max}$, and threshold power density P_{th} . System I is 38.4 Å InAs/17 Å Ga_{0.75}In_{0.25}Sb, system II is 30 Å InAs/20 Å Ga_{0.6}In_{0.4}Sb/50 Å InAs/33 Å Al_{0.6}Ga_{0.4}Sb/(11 Å InAs/27 Å Al_{0.6}Ga_{0.4}Sb)₄, and system V is a 18 Å InAs/21 Å AlAs_{0.15}Sb_{0.85}/18 Å InAs/27 Å Ga_{0.6}In_{0.4}Sb/18 Å InAs/21 Å AlAs_{0.15}Sb_{0.85}/18 Å InAs well surrounded by 4.5 periods of a 27 Å Al_{0.6}Ga_{0.4}Sb/11 Å InAs superlattice. The structures III, IV, and VI are described in Refs. 2, 3, and 12.

System	T (K)	E_g (μm)	$[(\gamma - \alpha_a)/P]_{\max}$ ($\mu\text{m}^2/\text{W}$)	P_{th} (kW/cm ²)	$(\gamma - \alpha_a)/\gamma$	
LWIR ACTIVE REGIONS $D_{\text{mode}} = 3.5 \mu\text{m}$, $\alpha_m + \langle \alpha_w \rangle = 60 \text{ cm}^{-1}$						
I	InAs/GaInSb	300	11	1.1×10^2	19	0.80
		77	7.5	1.6×10^4	0.13	
II	BGQW	300	11	4.7×10^3	0.45	0.93
		77	8	5.4×10^4	0.039	
III	Intersubband ^a		11	1.2×10^2	18	
IV	Intersubband ^b		11	27	78	
MWIR ACTIVE REGIONS $D_{\text{mode}} = 2.0 \mu\text{m}$, $\alpha_m + \langle \alpha_w \rangle = 10 \text{ cm}^{-1}$						
V	BGQW ^c	300	3.4	2.9×10^3	0.069	0.99
		77	3.0	3.0×10^4	0.0066	
VI	Intersubband ^d		3.6	9.7	21	

^aReference 2.

^bReference 3.

^cReference 11.

^dReference 12.

The net gain $[(\gamma - \alpha_a)/P]$ to volumetric power dissipation density ($P = JV_o$, where J is the volumetric recombination current density in the active region), is the only active region material parameter to appear in the first term of Eq. (2). The remaining parameters are related to the optical cavity and efficiency of electrical injection. When $[(\gamma - \alpha_a)/P]$ is maximized the threshold power is minimized. The net material gain to volumetric power appropriately weighs the importance to laser performance of the density of states, recombination rates, differential gain, and intersubband absorption within the active region. The difference between thickening a noncascade active region (or the individual stages of a cascade laser) and adding stages to a cascade laser is how I and V_{AR} change. Increasing the number of stages increases the voltage drop across the entire structure but not the current through it. In contrast, an increase in the thickness of a noncascade active region (or the individual stages of a cascade) increases the current through the structure but leaves the voltage drop unchanged. Both methods of increasing the thickness of the active region will *linearly* increase the dissipated power and also linearly increase the modal gain. Thus the ratio of gain to power dissipation density is an intensive quantity associated with all active regions, whether they are cascades or not.

The second term in Eq. (2) describes the power slope efficiency of the structure. The only active region parameter appearing here is $(\gamma - \alpha_a)/\gamma$. The power slope efficiency of the laser, unlike the current slope efficiency, is independent of the number of stages in a cascade. As will be noted below, this conclusion must be modified if the series resistance term dominates in Eq. (1).

Table I summarizes our results for several active regions. For LWIR interband active regions based on the InAs/GaInSb system we consider (I) an InAs/GaInSb superlattice and (II) an 11-layer structure further refined to balance the band-edge densities of states, reduce intersubband absorption, and reduce Auger recombination. The 300 K figure of

merit for the simple interband system I is comparable to that of the best 11 μm intersubband laser, system III, and exceeds that of system IV. At 300 K the calculated values for system II exceed by over an order of magnitude the current performance of LWIR intersubband active regions (systems III and IV). Two MWIR results are presented in Table I: system V is a 3.4 μm interband structure¹¹ whose 300 K figure of merit exceeds that of the 3.6 μm intersubband structure,¹² system VI, by over two orders of magnitude. At 77 K the performance of the interband devices improves dramatically, whereas the intersubband devices perform comparably to how they performed at 300 K. We emphasize these figures of merit are independent of the number of stages in a cascade. It is important to acknowledge, however, that aspects of device performance not considered here, such as vertical transport and thermal conductivity, could affect the relative performance of these active regions in actual devices. Also shown in Table I are the threshold input power densities for these systems based on cavity properties obtained from waveguiding calculations for typical designs in this wavelength range (several groups have achieved better cavity properties than these in this wavelength range). Finally the value of $(\gamma - \alpha_a)/\gamma$ at the optimum carrier density for the threshold figure of merit is shown at 300 K for the interband active regions. When operated at these carrier densities the material losses of these active regions are overwhelmed by the large material gains.

We now describe our calculations of the net material gain to volumetric power ratio, $[(\gamma - \alpha_a)/P]$, as a function of gain, first for intersubband structures and then for interband structures. The gain region of an intersubband laser can be modeled as a three-level laser in steady state. The principal characteristics of this system are $\mu_{21} = ez_{21}$, the dipole matrix element between the upper lasing state (2) and the lower lasing state (1), τ_1 and τ_2 , which are the total lifetimes of the two states, and τ_{21} , which is the scattering time from state 2 to state 1. These quantities are available from Refs. 2,

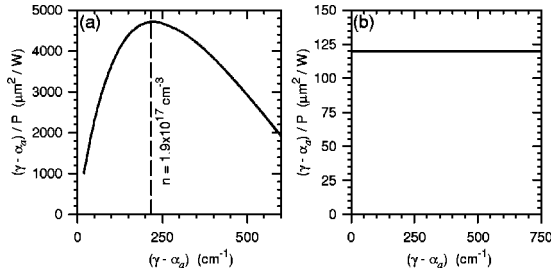


FIG. 1. Net gain per unit volumetric power dissipation density, $[(\gamma - \alpha_a)/P]$, as a function of net gain at 300 K for (a) system II and (b) system III. Note the different scales. The density corresponding to the optimum $[(\gamma - \alpha_a)/P]$ is indicated in (a). The net gain at this density is the optimum material net gain for this system.

3, 12; if τ_2 and τ_{21} are not both given we assume $\tau_2 = \tau_{21}$. We assume pumping only into state (2) and no thermal population of state (2). For such a system the gain¹³

$$\gamma = \left(\frac{2\pi^2 \nu g_\nu}{3hc n^5} \mu_{21}^2 \right) \frac{R \tau_2 [1 - (\tau_1/\tau_{21})]}{1 + (I/I_s)}, \quad (3)$$

where I_s is the saturation intensity, g_ν is the half width at half maximum (HWHM) of the gain linewidth, n is the index of refraction, I is the light-field intensity, h is Planck's constant, ν is the frequency of the light and c is its speed in vacuum. For an intersubband laser $R = J/e$, where J is the volumetric current density. Assuming that the optical loss in the active region is negligible and that the operating intensity is small compared to the saturation intensity

$$\frac{(\gamma - \alpha_a)}{P} = \frac{2\pi^2 e \nu g_\nu}{3n^5 hc} \frac{\mu_{21}^2 \tau_2 [1 - (\tau_1/\tau_{21})]}{V_o}. \quad (4)$$

For interband structures calculations of the net gain and the carrier recombination rate are performed with the full nonparabolic band structure and momentum-dependent matrix elements obtained from a 14-band bulk basis superlattice $\mathbf{K} \cdot \mathbf{p}$ formalism, where the problem is solved in momentum space in a way similar to Ref. 14 for an eight-band model. Input parameters¹⁵ to the calculation are limited to energy levels and matrix elements of bulk constituents, and the valence band offsets between layers. Results from such calculations have been in good agreement with experiment for optical properties¹⁶ and Auger rates¹⁷ in related type-II multilayer structures.

The figure of merit as a function of net material gain for systems II and III at 300 K is shown in Fig. 1. Note that the intersubband structure, system III, has a distinctly different shape than that of the interband structure, due to the linear dependence of the gain on the upper lasing state density and the assumed density-independent state-to-state scattering lifetimes. This contrasts with the interband structures where a minimum carrier density is required to achieve gain. The figure of merit for the intersubband structure should decrease at high gain due to an increase in τ_{21} from electron-electron scattering.¹⁸

We conclude with some brief comments on cascade versus noncascade designs. The "quantum defect" $h\nu/eV_o$ is

likely greater for noncascade than cascade structures. However, as we have defined it above, leakage of a carrier through even a single stage of a multistage cascade structure would reduce the injection efficiency for the device η_i , so η_i is likely to be greater for noncascade than cascade lasers. As a final point, the loss of input power associated with series resistance is quadratic rather than linear in the input current density, so if series resistance is significant, the power slope efficiency of noncascade structures may be reduced substantially relative to cascade structures. As an example, for a device with 0.1 mm^2 area and 0.25Ω series resistance, the calculated wall plug efficiency of a 25-stage active region based on structure III exceeds that of a noncascade design of structure II for output powers greater than 100 mW at 300 K. The wall plug efficiency of a 25-stage design of structure II will, however, always exceed that of a 25-stage design of structure III.

This research was supported in part by the U.S. Air Force, Air Force Materiel Command, Air Force Research Laboratory, Kirtland AFB, New Mexico, 87117-5777 (Contract No. F29601-97-C-0041) and the National Science Foundation (Grant No. ECS-9707799).

- ¹M. Tacke, *Infrared Phys. Technol.* **36**, 447 (1995).
- ²C. Sirtori, J. Faist, F. Capasso, D. L. Sivco, A. L. Hutchinson, and A. Y. Cho, *Appl. Phys. Lett.* **69**, 2810 (1996).
- ³G. Scamarcio, C. Gmachl, F. Capasso, A. Tredicucci, A. L. Hutchinson, D. L. Sivco, and A. Y. Cho, *Semicond. Sci. Technol.* **13**, 1333 (1998).
- ⁴D. H. Chow, R. H. Miles, T. C. Hasenberg, A. R. Kost, Y. H. Zhang, H. L. Dunlap, and L. West, *Appl. Phys. Lett.* **67**, 3700 (1995); T. C. Hasenberg, R. H. Miles, A. R. Kost, and L. West, *IEEE J. Quantum Electron.* **33**, 1403 (1997).
- ⁵J. I. Malin, J. R. Meyer, C. L. Felix, J. R. Lindle, L. Goldberg, C. A. Hoffman, and F. J. Bartoli, *Appl. Phys. Lett.* **68**, 2976 (1996).
- ⁶M. E. Flatté, T. C. Hasenberg, J. T. Olesberg, S. A. Anson, T. F. Boggess, C. Yan, and D. L. McDaniel, Jr., *Appl. Phys. Lett.* **71**, 3764 (1997).
- ⁷J. T. Olesberg, M. E. Flatté, C. H. Grein, T. C. Hasenberg, S. A. Anson, and T. F. Boggess, *Appl. Phys. Lett.* **74**, 188 (1999).
- ⁸See, e.g., L. A. Coldren and S. W. Corzine, *Diode Lasers and Photonic Integrated Circuits* (Wiley, New York, 1995).
- ⁹I. Vurgaftman, J. R. Meyer, and L. R. Ram-Mohan, *IEEE Photonics Technol. Lett.* **9**, 170 (1996).
- ¹⁰R. Q. Yang and S. S. Pei, *J. Appl. Phys.* **79**, 8197 (1996).
- ¹¹J. T. Olesberg, M. E. Flatté, T. C. Hasenberg, and C. H. Grein (unpublished).
- ¹²J. Faist, F. Capasso, D. L. Sivco, A. L. Hutchinson, S.-N. G. Chu, and A. Y. Cho, *Appl. Phys. Lett.* **72**, 680 (1998).
- ¹³See, e.g., J. T. Verdeyen, *Laser Electronics*, 3rd ed. (Prentice-Hall, Englewood Cliffs, NJ, 1995).
- ¹⁴R. Winkler and U. Rössler, *Phys. Rev. B* **48**, 8918 (1993).
- ¹⁵Parameters for the systems considered come from Landolt-Börnstein: *Physics of Group IV Elements and III-V Compounds*, edited by O. Madelung (Springer, New York, 1982), Vol. III, p. 17a, and Landolt-Börnstein: *Intrinsic Properties of Group IV Elements and III-V, II-VI, and I-VII Compounds*, edited by O. Madelung (Springer, New York, 1987), Vol. III, p. 22a.
- ¹⁶J. T. Olesberg, S. A. Anson, S. W. McCahon, M. E. Flatté, T. F. Boggess, D. H. Chow, and T. C. Hasenberg, *Appl. Phys. Lett.* **72**, 229 (1998).
- ¹⁷M. E. Flatté, C. H. Grein, T. C. Hasenberg, S. A. Anson, D.-J. Jang, J. T. Olesberg, and T. F. Boggess, *Phys. Rev. B* **59**, 5745 (1999); D.-J. Jang, M. E. Flatté, C. H. Grein, J. T. Olesberg, T. C. Hasenberg, and T. F. Boggess, *Phys. Rev. B* **58**, 13047 (1998).
- ¹⁸P. Hylgaard and J. W. Wilkins, *Phys. Rev. B* **53**, 6889 (1997).